Journal of Applied Electrochemistry (2006) 36:745–757
DOI 10.1007/s10800-006-9121-3

A novel approach for computing tertiary current distributions based on simplifying assumptions

VIJAYASEKARAN BOOVARAGAVAN[1,2] and C. AHMED BASHA[1,*]
[1]*Central Electrochemical Research Institute, Karaikudi, Tamilnadu, 630006, India*
[2]*Department of Chemical Engineering, Tennessee Technological University, Cookeville, TN, 38505, USA*
*(*author for correspondence tel.: +91-4565-227550, fax: +91-4565-227713, E-mail: basha@cecri.res.in)*

Received 10 June 2005; accepted in revised form 13 January 2006

Key words: convective transport, electrochemical cell, electrode kinetics, mathematical analysis, tertiary current distributions

Abstract

A novel yet efficient method for the computation of simplified tertiary current density and surface concentration distributions in electrochemical processes is presented. The method is rooted in the important physiochemical property that the activation potential is constant and uniform for given electrode material during the electrolysis. The technique is attractive because it involves a single iterative procedure against the conventional doubly iterative procedure. The initial assumption of current distribution along the electrode is also not necessary, as it involves only an assumption of a suitable power series to solve steady state laminar convective diffusion. Accordingly the method is relevant only for electrodes of constant activation polarization, but this holds good for situations where the electrode configurations are such that the primary current density distribution is almost uniform and for situations where the Wagner number is high. To illustrate the utility of the technique the procedure is applied to some realistic problems encountered in electrochemical engineering such as the current distribution either in plane-parallel plate electrode with electrolyte flowing between them or a moving electrode with the electrolyte stationary.

1. Introduction

The knowledge of current distribution in various geometrical configuration of electrolytic cells is important both for the analysis of data obtained in electrochemical experiments and also for design and scale-up. Owing to the large number of variables, the nature of the problem is complex. However, several situations for limited validity can be analyzed with comparative ease such as the primary and secondary current distributions. In order to design a reactor and also to understand the performance in this more complicated process, it is essential to simultaneously take into account several phenomena that influence the current distribution. Thus, it is necessary to solve for the concentration fields and the potential field simultaneously. The solution of such problems is often termed the tertiary current distribution. Since the mathematical methods leading to an analytical solution are usually not applicable in more complicated cases, the only possibility remaining is to use a numerical or semi-analytical approach.

Tertiary current distributions have not been treated extensively. Newman [1] has discussed this class of problem, indicating how to treat current distribution in cells where the potential distribution in the bulk of the solution and the concentration distribution in the diffusion layer must be calculated simultaneously. These ideas [2] were applied to other electrochemical cell geometries such as current distribution on plane-parallel electrodes, rotating spherical electrodes, continuous moving sheet electrodes etc., The computation methods used in most of these cases are one or the other form of Newman's technique. Nowadays finite element or finite difference methods provide an option to model electrochemical systems. In recent work [3–7] semi-analytical methods or numerical methods have been used for calculating current density distributions with respect to diffusion, migration and laminar convection, including high velocities and electrochemical reactions of exponential kinetics.

In this work, the authors propose a new semi-analytical method with minimum number of iterative procedures and assumptions that are needed to represent the simplified tertiary current distribution. Although the proposed technique for the computation of tertiary current distribution brings in mind Newman's technique, this method involves a single iterative procedure. Newman's technique is double iterative and also involves the initial assumption of current distribution itself. The technique is much simpler as it assumes only an appropriate power series for surface concentration and makes use of the augmented Butler–Volmer

equation for calculating the coefficients of the assumed series. The basis of this evaluation is rooted in a strong physiochemical fact that activation polarization remains constant throughout the electrode surface.

Thus extent possible analytical expressions used during the computation give much insight into the system, which is one of the primary objectives of modeling. Certainly the developed method is not a solution for all problems but holds good within the stated limitations.

2. Mathematical analysis

A simple model considered for the evaluation of tertiary current distributions involves the following assumptions: (a) a single cathodic reaction takes place at the cathode; (b) the concentration overpotential and the activation overpotential at the counter electrode are zero; (c) the transport and kinetic parameters do not vary in space or time; (d) the presence of cell wall and the counter electrode do not affect the flow boundary layer on the working electrode; and (e) the physical properties of the electrolyte are constant and the cathode is of primary interest.

2.1. *Voltage balance*

Assuming that we impose a specific voltage drop E across the electrodes; the overall voltage balance may be written as

$$E = \phi_{\text{ohm}} + \eta_{\text{a}} + \eta_{\text{c}} \tag{1}$$

Here E is the difference between the applied cell voltage and the thermodynamic equilibrium cell voltage. ϕ_{ohm} is the ohmic voltage drop, η_{a} and η_{c} are the voltage drops due to activation polarization (i.e., kinetic effects) and concentration polarization (due to concentration gradients between the electrode surface and the bulk electrolyte) respectively.

2.2. *Modified Butler–Volmer electrode kinetics*

The polarization equation is necessary to express the dependence of the local rate of the reaction on the various concentrations and on the potential jump at the interface. It is common to use the Butler–Volmer equation of electrode kinetics of the form for metal/ion systems.

$$i = i_0 \left(\frac{C_{\text{s}}}{C_\infty}\right)^{\gamma} \left[\exp\left(\frac{\alpha n F}{RT}\eta_{\text{a}}\right) - \exp\left(-\frac{\beta n F}{RT}\eta_{\text{a}}\right)\right] \tag{2}$$

where i_0 is the exchange current density and α,β and γ are kinetic parameters.

2.3. *Concentration overpotential*

In view of the assumption of an excess of supporting electrolyte the potential difference associated with the concentration variation is written in terms of concentration overpotential as commonly followed.

2.4. *Convective diffusion*

The diffusion process is governed by a partial differential equation that describes the way that the concentration of the electrochemically active species changes with respect to the distance along the working electrode. Then the steady-state laminar convective diffusion equation, $V(\nabla C) = D\nabla^2 C$ is used to describe the transport of the reactive ion from the bulk to the electrode surface. The choice of spatial coordinate and the boundary conditions depend on the electrode geometry.

2.5. *Laplace equation*

In the interior of an electrolytic cell, there are no free electrical charges. The ohmic potential drop across the concentration boundary layer is negligibly small compared to the ohmic potential drop across the bulk of the electrolyte. Therefore, the potential drop across the electrolyte is governed by the Laplace equation, $\nabla^2\phi$ where $\phi(x,y)$ represents the local electrical potential.

Thus to determine the current density and concentration distributions along the electrode, the convective diffusion equation and the Laplace equation must be solved simultaneously along with electrochemical kinetics using suitable geometry-dependent boundary conditions. Thus there are five equations; these equations are strongly coupled algebraic-differential equations and simultaneous solution is required to find the unknowns namely, activation polarization, concentration overpotential, ohmic potential drop, surface concentration and local current density at the electrode.

3. Semi-analytical method

Many electrochemical systems require common calculation procedures to analyze tertiary current distribution irrespective of the cell geometry. The working electrode may take a different position with respect to the counter electrode such as a rectangular geometry where the electrodes are parallel or through-hole plating where the electrodes are perpendicular. The basic computation methodology developed here is based on this constant and uniform activation polarization property of the electrode and power series solution assumption for convective diffusion. The main principle of the calculation procedure, consists in assuming the series solution for the surface concentration and in finding out the expressions for evaluating the series coefficients. A scaling of all parameters that appear in the problem suggests that the results can be best presented in terms of the dimensionless quantities.

$$X = \frac{x}{L}; \quad b^* = \frac{b}{L}; \quad C_s^* = \frac{C_s}{C_\infty}; \quad i^* = \frac{nF}{RT}\frac{L}{k}i$$
$$Q^* = \frac{nF}{RT}Q, \quad \text{where } Q = \eta_a,\ \eta_c,\ \phi_{ohm},\ E \tag{3}$$

The calculation procedure for the more general case discussed in the previous section is presented below. Introducing the dimensionless quantities into the governing model equations, we have

Voltage Balance

$$E^* = \phi_{ohm}^* + \eta_a^* + \eta_c^* \tag{4}$$

modified Butler–Volmer electrode kinetics

$$i^* = JC_s^{*\gamma}\left[\exp\left(\alpha\eta_a^*\right) - \exp\left(-\beta\eta_a^*\right)\right] \tag{5}$$

The transfer coefficients α and β are usually 0.5. The parameter γ is the electrochemical reaction order and it is 0.5. J is the dimensionless exchange current density and represents the ratio of the ohmic potential drop to the activation overpotential.

Concentration overpotential

$$\eta_c^* = \ln C_s^* \tag{6}$$

The analytical solution of the steady-state laminar convective diffusion can be obtained in three steps. (i) Apply Laplace transformation to convective diffusion assuming that the velocity component for the electrolyte along the y-direction is negligible; (ii) Solve the resulting linear second-order ordinary differential equation with the corresponding boundary conditions of the given geometry; and (iii) Use the convolution theorem and take inverse Laplace transformation to get the complete solution. The resulting expression that relates the variables surface concentration and the local current density can be expressed as

$$i^*(X) = N\int_0^X \left(\frac{dC_s^*}{dX}\right)_{X=t} \frac{dt}{(X-t)^q} \tag{7}$$

where t is a dummy variable, q is a geometric factor and can have any value smaller than one ($0<q<1$). It is heuristic, but appropriate if we choose the value based on the analytical expression of concentration field. For a semi-infinite plate $q=0.5$, for a parallel plate or flow through pipe $q=1/3$ (Leveque type equation) and for turbulent flow $q=0.8$ (Wilson type plot). N is a significant parameter called the average dimensionless limiting current density. Both q and N depend upon the cell geometry and the corresponding boundary conditions used. The dimensionless form of the Laplace equation can be written as

$$\nabla^2\phi^* = 0 \tag{8}$$

The effect of surface concentration on the reaction rate plays an important role in many electrochemical systems [8–10] such as batteries and electrochemical synthesis. To solve this system of equations (Eqs. (4)–(8)), we have stated with the assumption of a power series for the surface concentration as follow:

$$C_s^* = \sum_{n=0}^{\infty} a_n X^{nq} \tag{9}$$

Using the condition $C_s(0) = C_\infty$ i.e., the bulk concentration of the reacting species, the series coefficient $a_0 = 1.0$. Taking the first derivative of Eq. (9) with respect to X, the current density distribution can also be expressed in terms of an assumed power series using Eq. (7)

$$i^*(X) = N\sum_{n=1}^{\infty} n a_n q X^{(n-1)q}\beta(1-q, nq) \tag{10}$$

The modified Butler–Volmer electrode kinetics can be equated to the above series equation. The resulting expression is then used to calculate the numerical value of the other series coefficients. The expression is

$$JC_s^{*\gamma}\left[\exp\left(\alpha\eta_a^*\right) - \exp\left(-\beta\eta_a^*\right)\right] = N\sum_{n=1}^{\infty} n a_n q X^{(n-1)q}\beta(1-q, nq) \tag{11}$$

or

$$J\left[\sum_{n=0}^{\infty} a_n X^{nq}\right]^{\gamma}\left[\exp\left(\alpha\eta_a^*\right) - \exp\left(-\beta\eta_a^*\right)\right] = N\sum_{n=0}^{\infty}(n+1)a_{n+1} q X^{nq}\beta(1-q, (n+1)q) \tag{12}$$

The procedure for evaluating series coefficients and thus the concentration and current distributions is detailed in the Appendix for the case of a continuous moving sheet electrode process. Figure 1 illustrates the technique in more detail. Despite the nested iterations, the convergence is very rapid. The major differences and advantages of this procedure are

1. The developed method involves iteration for only one variable instead of doubly iterative calculation procedure used in the conventional methods.
2. The assumption of a power series solution for C_s^* alone is required in the present method unlike the initial guess of the current distribution itself.
3. Above all, the developed technique will open up the possibilities of modeling systems with irregular geometry, unusual boundary conditions or multi-ion electrodeposition.

The second striking feature enables a very simple programming need for this methodology. This capability becomes very important because, if the tertiary current distribution is the main issue, the assumption of current density distribution can produce coding intricacy and conspicuous errors. However, the method is still restricted to constant and uniform electrode material activation polarization. These features should also be taken into consideration for the applicability of the above semi-analytical method.

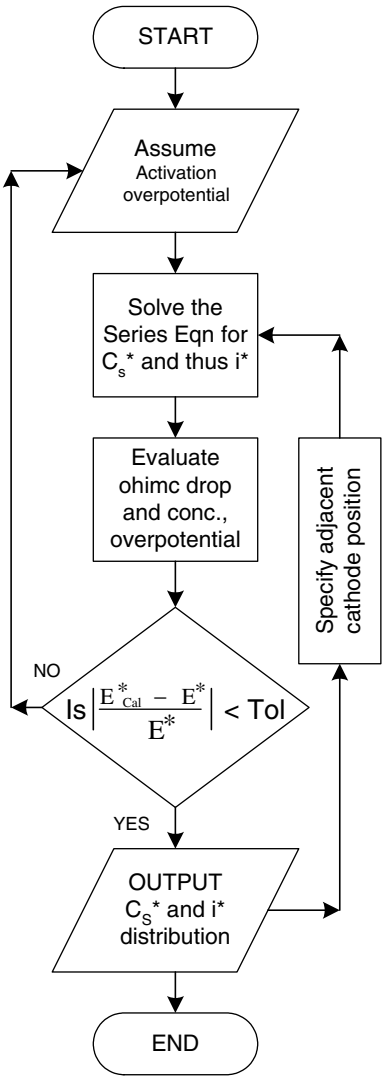

Fig. 1. Outline of the developed algorithm used to solve model equations.

The above method computes simplified tertiary current density and surface concentration distributions. For example the migration contribution to the transport mechanism of the reacting (and other) species has been ignored for adaptability purposes of the semi-analytical technique. However, the migration contribution may become important in not so dilute solutions and inside occluded geometries such as cavities, crevices, through holes, etc. In such cases Laplace's equation cannot accurately define the ohmic drop, the migration term that combines concentration and solution potential interactions should be included in the transport equation and, due to its strong non-linearity, only a numerical solution is feasible. Also it is not possible to catch edge effects on downstream electrode edges where singularities occur. Plating through holes requires simulation of the moving boundary developed at the plating electrode surface; but the present method attempts to attack a very complicated process with a rather basic approach. The case of plating through holes is an example of the necessity of a numerical approach. The other restrictions include that the method can hold well only when the convection is in the x and diffusion in the y and constant diffusivities. The method can also be easily extended even for other semi-analytical solutions [4] in the case of non-analytical solutions for the potential distribution. Also the method can handle well-defined non-constant velocities as long as the Laplace transform technique works. Thus, the numerical procedure addresses coupled phenomena for all ranges of simplified electrochemical systems. However, the applicability of the semi-analytical method is restricted for simulations of the changing current distribution and resulting electrode shape change in the transient problems. On the other hand, cases involving multiple species can be simulated based on the mass conservation equation.

4. Results and discussion

The proposed approach is general and, under the fitness of the mathematical formulation described in Section 2, the technique accounts for all possible configurations and operational alternatives of the electrochemical system. In the following section, the ease of use and the broad applicability of the presented algorithm are illustrated in three different electrochemical processes. The results are presented by solving the problems in terms of different dominant parameters.

4.1. *Continuous moving sheet electrode*

Electrochemical processes such as electrolysis of brine and electroplating of sheet metals and wires [11] make use of continuous moving electrodes. Consider one side of a continuous semi-infinite flat sheet electrode moving with a constant velocity U_s, through an otherwise undisturbed electrolyte as shown in the Figure 2. The sheet enters the cell through a watertight slot at one end of the cell and leaves the cell at the opposite side through a second slot. The motion of the solid surface

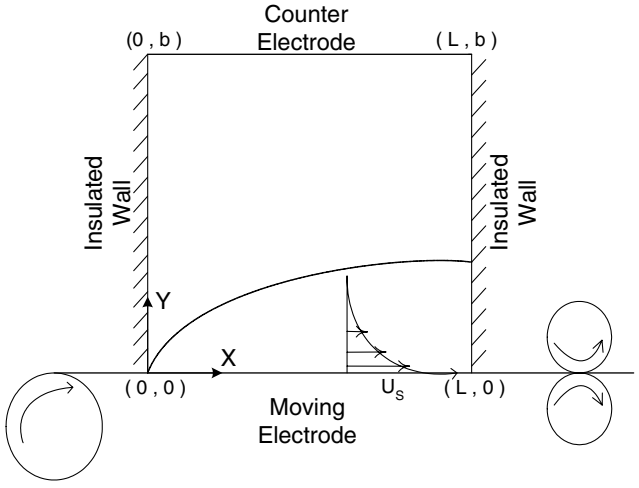

Fig. 2. Schematic diagram of a continuous moving sheet electrode process.

induces a flow of electrolyte in the direction of the sheet. The electrode velocity is high so that the boundary layer approximation can be used to describe the electrolyte flow near the surface. The steady-state laminar convective diffusion equation for a continuous moving sheet is

$$U\frac{\partial C}{\partial x}+V\frac{\partial C}{\partial y}=D\frac{\partial^2 C}{\partial y^2} \tag{13}$$

The boundary conditions at the walls, the anode ($y=b$) and the cathode ($y=0$) are $C(0, y)=C(x, \infty)=C_\infty$

$$D\left.\frac{\partial C(x,y)}{\partial y}\right|_{y=0}=\frac{i(x)}{nF} \tag{14}$$

Assuming that the variation in V is negligible and applying Laplace Transformation (i.e., x to p in C), the complete solution of Eq. (13) using the above boundary conditions is

$$C(p,0)=\frac{C_\alpha}{p}-\frac{1}{nF\sqrt{DU}}\frac{i(p)}{\sqrt{p}} \tag{15}$$

Using the convolution theorem, the inverse Laplace transform of Eq. (15) gives the surface concentration or the local current density distribution along the surface of the continuous moving sheet electrode, expressed as

$$C(x,0)=C_\infty-\frac{1}{nF\sqrt{\pi DU_s}}\int_0^x\frac{i(t)}{\sqrt{x-t}}\,\mathrm{d}t \tag{16}$$

or

$$i(x)=nF\sqrt{\frac{DU_s}{\pi}}\int_0^x\left(\frac{\mathrm{d}C}{\mathrm{d}x}\right)_{x=t}\frac{\mathrm{d}t}{\sqrt{x-t}} \tag{17}$$

Introducing the dimensionless parameter Eq. (3) into the above equation, the resulting expression for the variable surface concentrations at the electrode is

$$\begin{aligned} i^*(X)&=N\int_0^X\left(\frac{\mathrm{d}C_s^*}{\mathrm{d}X}\right)_{X=t}\frac{\mathrm{d}t}{\sqrt{(X-t)}}\\ &=N\sum_{n=1}^{\infty}\frac{n}{2}a_nX^{\frac{n-1}{2}}\beta\left(\frac{n}{2},\frac{1}{2}\right)\end{aligned} \tag{18}$$

where

$$N=\frac{-n^2F^2DC_\infty}{RTk\sqrt{\pi}}\sqrt{\mathrm{ReSc}}=\frac{2\sqrt{X}}{\pi}\int_0^1 i_{\lim}^*\mathrm{d}X$$

Here the assumed series solution for C_s^* is

$$C_s^*=\sum_{n=0}^{\infty}a_nX^{\frac{n}{2}} \tag{19}$$

The following boundary conditions are used to solve the potential field expressed by the Laplace equation,

$$\frac{\partial\phi}{\partial x}=0 \quad \text{at } x=0 \text{ and } x=1 \quad \text{for } 0\le y\le b \tag{20a}$$

$$\phi=0 \quad \text{at } y=b \quad \text{for } 0\le x\le L \tag{20b}$$

$$\frac{\partial\phi}{\partial y}=\frac{-i}{k} \quad \text{at } y=0 \quad \text{for } 0\le x\le L \tag{21}$$

The Laplace equation have been solved by the method of separation of variables using the above boundary conditions and the solution for the ohmic potential drop across the cell is expressed in terms of a Fourier cosine series.

$$\begin{aligned}\phi_{\mathrm{ohm}}^*=b^*\int_0^1 i^*\mathrm{d}t+\sum_{m=1}^{\infty}\frac{2}{m\pi}\tan h(m\pi b^*)\cos(m\pi X)\\ \int_0^1 i^*\cos(m\pi t)\mathrm{d}t\end{aligned} \tag{22}$$

The governing equations describing an electrochemical process at the moving electrode are given in Table 1 and simulation data are reported in Table 4. Here Re and Sc are Reynolds and Schmidt number, respectively. In addition, the dimensionless parameters N, J and b^* are subjected to variation to examine their influence. The dimensionless average limiting current density N, represents the ratio of ohmic potential drop to the concentration overpotential at the electrode.

The model equations are solved numerically. Figure 3a shows the current distributions at various current levels for $N=100$, $J=1$ and $b^*=1$. The vertical axis is the local current density divided by the average current density at the electrode. The horizontal axis is the dimensionless surface distance from the entrance point of the moving electrode. It is seen that at a low current level the current distribution profile is almost flat. This is because the concentration polarization is small due to negligible mass-transfer resistance. As the current increases, the profile has a pronounced steep region near the leading edge and linearly drops thereafter. The current density is highest at the leading edge where the concentration boundary layer is thin and the rate of mass transfer is high. Then the concentration boundary layer grows gradually from the leading edge and the current density decreases. At the trailing edge, the effect of the concentration boundary layer is greater and the current density becomes less than the average value.

Figure 3b presents the surface concentration profiles for different currents. The concentration effects increase with current density due to mass transfer limitations.

Table 1. Simplified model equations for moving electrode process

	Moving electrode process
Voltage balance	$E^* = \phi^*_{\text{ohm}} + \eta^*_a + \eta^*_c$
Electrode kinetics	$i^* = JC^{*\gamma}_s\left[\exp(\alpha\eta^*_a) - \exp(-\beta\eta^*_a)\right]$ where $J = \frac{nFL}{RTk} i_0$
Concentration overpotential	$\eta^*_c = \ln C^*_s$
Ohmic potential drop	$\phi^*_{\text{ohm}} = b^* \int_0^1 i^* \mathrm{d}t + \sum_{m=1}^{\infty} \frac{2}{m\pi} \tan h(m\pi b^*) \cos(m\pi X) \int_0^1 i^* \cos(m\pi t)\mathrm{d}t$
Convective diffusion	$i^*(X) = N \int_0^X \left(\frac{\mathrm{d}C^*_s}{\mathrm{d}X}\right)_{X=t} \frac{\mathrm{d}t}{\sqrt{(X-t)}} = N \sum_{n=1}^{\infty} \frac{n}{2} a_n X^{\frac{n-1}{2}} \beta\left(\frac{n}{2}, \frac{1}{2}\right)$
	where $N = \frac{-n^2F^2DC_\infty}{RTk}\sqrt{\pi}\sqrt{\text{ReSc}} = \frac{2\sqrt{X}}{\pi}\int_0^1 i^*_{\text{lim}}\mathrm{d}X$,
	$\text{Re} = \frac{U_s L}{\nu}$ & $\text{Sc} = \frac{\nu}{D}$

The surface concentration is equal to the bulk concentration at the leading edge and decreases sharply with increasing distance along the electrode. The surface concentration distribution is most uniform for the smallest current. Figure 4a shows the effect of average dimensionless limiting current density, N, on the current distribution at $J = 100$ and $b^* = 1$. For large values of N, the current densities exceed the limiting current density locally near the leading edge as the mass transfer proceeds faster and the current distribution becomes more uniform. The other dimensionless parameter, the exchange current density, is not so important because the numerical investigation on different values of J ranging from 0.001 to 100 indicates that, for large values of N, the effect of J is smaller; in general for more uniform current distribution the value of J should be smaller.

The next stage of the analysis for uniform current density distribution is to study the effect of electrode spacing at the continuous moving electrode. Figure 4b shows that the current density becomes more uniform as the value of b^* increases. But increase in b^* poses the question of economic viability; the effect is more pronounced when N is large. Thus for uniform current distribution, b^* can be increased for low values of N. However, for very low values of N, the process tends to be mass transfer limited. Model equations give a better solution for the system with N greater than 200. This condition of large N is imposed by low electrolytic conductivity and high limiting current density. Most industrial electrochemical processes are carried out under this condition of large N. In electrowinning of copper-containing minerals the acidic copper sulfate bath contains 0.75 M $CuSO_4$ and 1 M H_2SO_4 with a specific conductivity of 0.4 mho cm^{-1} [12] at room temperature. Thus for a cell 4 m long and with sheet velocity 0.026 m s^{-1}, the value of N for copper deposition is 1610 at 25 °C.

4.2. *Electroplating of a through-hole*

We now consider the electroplating of high aspect ratio through-holes as shown in Figure 5. Plating inside through-holes and crevices is critically important for innumerable technological applications [13]. High-density circuits require thicker boards with longer, smaller diameter holes. These trends make it difficult to achieve uniform plating due to severe mass-transfer limitations [14]. The steady-state diffusion equation for laminar convective diffusion in circular cylindrical coordinates can be written as

$$V_z(r)\frac{\partial C}{\partial z} = D\left[\frac{\partial^2 C}{\partial r^2} + \frac{1}{r}\frac{\partial C}{\partial r}\right] \tag{23}$$

Here r and z are radial and axial distances. For small values of z such that $zD/2\langle V_z\rangle R_0^2 < 0.01$, Leveque [15] recognized that there is a diffusion layer near the tube wall where the second term in the brackets of Eq. (23) becomes much smaller than the first and the electrolyte velocity is approximately linear with distance from the tube wall. By inserting these approximations into Eq. (23), one obtains

$$V_z(y)\frac{\partial C}{\partial z} = D\frac{\partial^2 C}{\partial y^2} \quad \text{where } V_z(y) = \frac{4\langle V_z\rangle}{R_0} y$$

where y is the normalized radial distance from the through-hole wall $y = (R_0 - r)$ and $\langle V_z \rangle$ is the average electrolyte velocity in the axial direction. Under these situations the boundary conditions are

$$\begin{aligned} &C = C_\infty \quad \text{at } y = \infty \quad \text{for } z0 \\ &C = C_\infty \quad \text{at } 0 \le y \le \infty \quad \text{for } z \le 0 \\ &\frac{\partial C}{\partial y} = \frac{i(z)}{nFD} \quad \text{at } y = 0 \quad \text{for } 0 \le z \le L \end{aligned} \tag{24}$$

The resulting expression for surface concentration and average dimensionless limiting current density is

$$i^* = N\int_0^X \left(\frac{\mathrm{d}C^*_s}{\mathrm{d}X}\right)_{X=t} \frac{\mathrm{d}t}{\sqrt{[3]x - t}} = N\sum_{n=1}^{\infty} \frac{n}{3} a_n X^{\frac{n-1}{3}} \beta\left(\frac{n}{3}, \frac{2}{3}\right) \tag{25}$$

$$N = \frac{2n^2F^2DC_\infty L^2}{\Gamma\left(\frac{4}{3}\right)RTkR_0}\left(\frac{4\langle V_z\rangle}{9R_0DL}\right)^{\frac{1}{3}}$$

In Eq. (25) $X = y/L$, the dimensionless through-hole axial distance. The polynomial series solution assumed for the dimensionless surface concentration is

$$C_s^* = \sum_{n=0}^{\infty} a_n X^{\frac{n}{3}} \tag{26}$$

The Laplace equation is solved using the following boundary conditions

$$\begin{aligned} &\frac{\partial \phi}{\partial r} = 0 \ \text{ at } z = 0 \text{ and } z = L \ \text{ for } 0 \le r \le R_0 \\ &\frac{\partial \phi}{\partial r} = \frac{-i(z)}{k} \ \text{ at } 0 < z < L \text{ and } r = R_0 \end{aligned} \tag{27}$$

The analytical expressions in Table 2 describe mass transfer of reacting species, ohmic resistance in the electrolyte phase and charge transfer at the through-hole wall. Here I_0 and I_1 are modified Bessel functions.

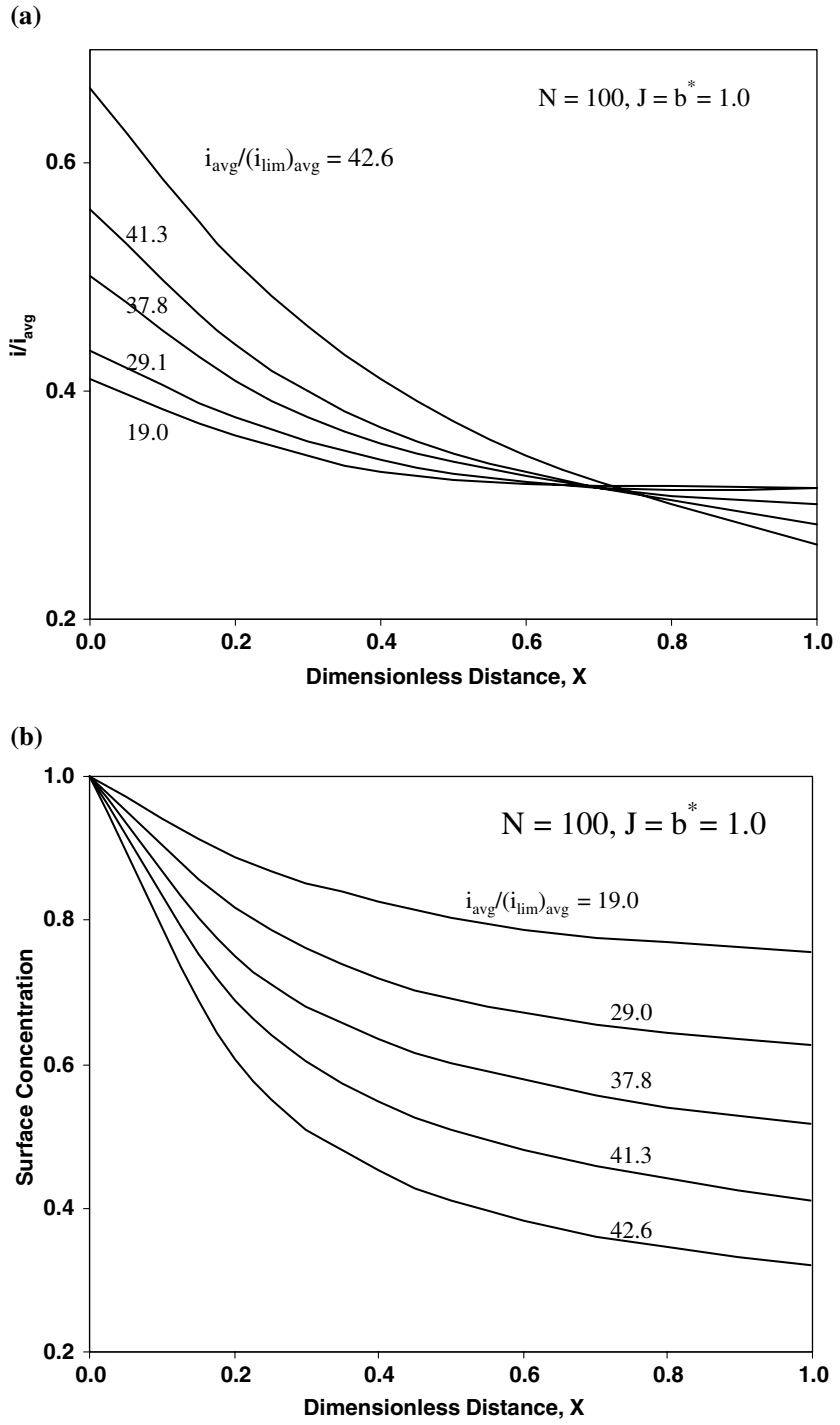

Fig. 3. (a) Current density distribution on the moving sheet electrode at various current levels and (b) Typical profiles of dimensionless surface concentration distribution on the continuous moving sheet electrode.

Typical electrolyte, kinetic, mass transfer and geometric parameters encountered during copper deposition are given in Table 4. The through-hole dimensions investigated correspond to aspect ratios of 10:1, 5:1 and 2:1. We assume symmetry of anode position and agitation on both sides of the board.

Figure 6a is the graphical representation of calculated dimensionless surface concentration distributions at various levels of polarization for the aspect ration 2:1 ($L = 0.8$ cm, $R_0 = 0.2$ cm), where the local current density is non-dimensionalized with respect to the average current density, i_{avg}. At relatively low values of applied potential, the current distribution depends on the cell geometry, the charge transfer characteristics of the electrochemical reaction and the electrolyte conductivity. As the applied potential is increased, the solution inside the through-hole becomes depleted in the reacting species. Consequently, the edges of the through-hole are more accessible to the counter electrode and are constantly being supplied with the reacting species. This

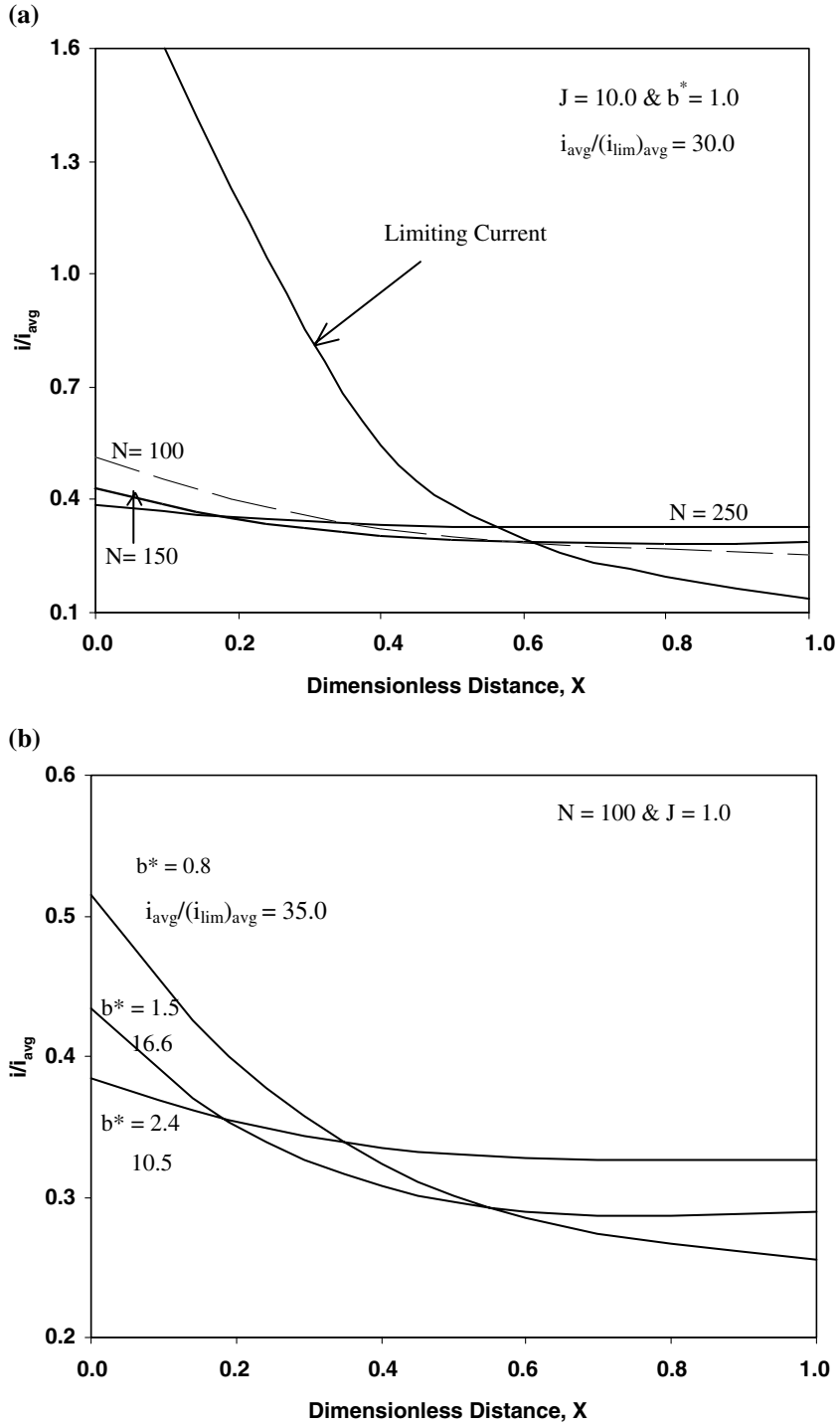

Fig. 4. (a) Effect of N on the current distribution for $J = b^* = 1.0$ and (b) Effect of electrode spacing on the current distribution at the continuous moving electrode.

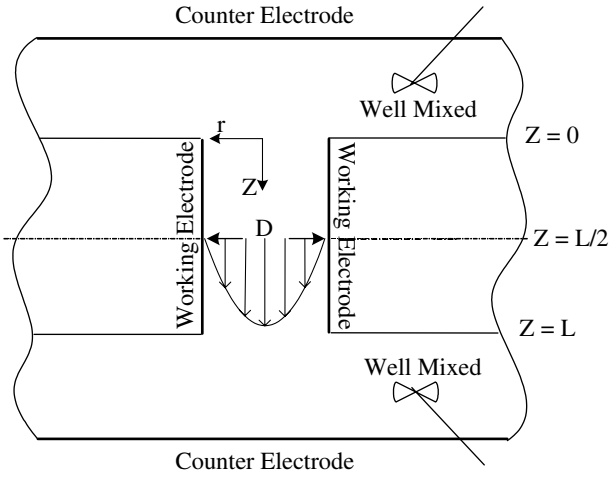

Fig. 5. Definition sketch of a through-hole system under consideration.

causes the current distribution to become increasingly non-uniform, as shown in Figure 6b.

As the through-hole radius becomes smaller and the aspect ratio becomes higher, the more acute the problem will be. At relatively low values of applied potential, the current distribution will become more non-uniform with decreasing hole radius due to geometric considerations. At high-applied potentials this trend will continue because of the increase in mass-transfer restriction with decreasing hole radius. This is illustrated in Figure 6c for through-holes with aspect ratio 2:1 ($L = 0.8$ cm, $R_0 = 0.2$ cm), 5:1 ($L = 0.8$ cm, $R_0 = 0.08$ cm) and 10:1 ($L = 0.8$ cm, $R_0 = 0.04$ cm).

4.3. *Plane-parallel electrodes*

Because of the importance of parallel electrodes, a great deal of effort has been devoted to describing the current

Table 2. Simplified model equations for through-hole plating process

	Through-hole plating process
Voltage balance	$E^* = \phi^*_{\text{ohm}} + \eta^*_{\text{a}} + \eta^*_{\text{c}}$
Electrode kinetics	$i^* = JC^{*\gamma}_{\text{s}}\left[\exp(\alpha\eta^*_{\text{a}}) - \exp(-\beta\eta^*_{\text{a}})\right]$ where $J = \frac{2nFL^2}{RTkR}\,i_0$
Concentration overpotential	$\eta^*_{\text{c}} = \ln C^*_{\text{s}}$
Ohmic potential drop	$\phi^*(\xi) = \phi^* - \sum_{n=1}^{\alpha}\sin(\lambda_n\xi)\left[\frac{\ell}{n\pi}\frac{I_0(\lambda_n\ell)}{I_1(\lambda_n\ell)}\int_0^1 i^*(\xi)\sin(\lambda_n\xi)\mathrm{d}\xi\right]$ where $\ell = \frac{R_0}{L}$ and $\lambda_n = n\pi$
Convective diffusion	$i^* = N\int_0^X \left(\frac{\mathrm{d}C^*_{\text{s}}}{\mathrm{d}X}\right)_{X=t}\frac{\mathrm{d}t}{\sqrt{[3]x - t}} = N\sum_{n=1}^{\infty}\frac{n}{3}a_nX^{\frac{n-1}{3}}\beta\left(\frac{n}{3},\frac{2}{3}\right)$ where $N = \frac{2n^2F^2DC_\infty L^2}{\Gamma\left(\frac{4}{3}\right)RTkR_0}\left(\frac{4\langle V_z\rangle}{9R_0DL}\right)^{\frac{1}{3}}$

Table 3. Simplified model equations for plane-parallel electrode process

	Plane-parallel electrode process
Voltage balance	$E^*_{\text{cath}} = \phi^*_{\text{ohm,cath}} + \eta^*_{\text{a,cath}} + \eta^*_{\text{c,cath}}$
Electrode kinetics	$i^*_{\text{cath}} = JC^{*\gamma}_{\text{s}}\left[\exp\left(\alpha\eta^*_{\text{a,cath}}\right) - \exp\left(-\beta\eta^*_{\text{a,cath}}\right)\right]$ where $J = \frac{nFL}{RTk}\mathrm{i}_0$
Concentration overpotential	$\eta^*_{\text{c,cath}} = \left\{\ln C^*_{\text{s}} - t(1 - C^*_{\text{s}})\right\}$
Ohmic potential drop	$\phi^*_{\text{ohm,cath}} = \phi^* - \frac{1}{2\pi}\int_0^1\left\{i^*_{\text{cath}}\ln\left[\sin h^2\frac{\pi b^*(X-t)}{2}\right] + i^*_{\text{anode}}\ln\left[\cos h^2\frac{\pi b^*(X-t)}{2}\right]\right\}\mathrm{d}t$
Convective diffusion	$i^* = N\int_0^X \left(\frac{\mathrm{d}C^*_{\text{s}}}{\mathrm{d}X}\right)_{X=t}\frac{\mathrm{d}t}{(X-t)^{\frac{1}{3}}} = N\sum_{n=1}^{\infty}\frac{n}{3}a_nX^{\frac{n-1}{3}}\beta\left(\frac{n}{3},\frac{2}{3}\right)$ where $N = \frac{-n^2F^2DC_\infty}{(1-\mathrm{t})\mathrm{RTk}}\frac{1}{\Gamma\left(\frac{4}{3}\right)}\left(\frac{2\langle U\rangle L^2}{3Db}\right)^{\frac{1}{3}}$

Table 4. Physicochemical and kinetic parameters employed in model simulation

Parameter	Symbol	Value	References
Conductivity of bulk solution	κ	0.4 mho cm^{-1}	[2]
Diffusivity of copper	D	5.2$\times$ 10^{-6} cm^{2}s^{-1}	[2]
Cathodic transfer coefficient	β	0.5	[2]
Anodic transfer coefficient	α	0.5	[2]
Electrochemical reaction order	γ	0.5	[2]
Cell temperature	T	303 K	[2]
Exchange current density	i_0	1.0 mA cm^{-2}	[2]
Bulk concentration of reactant	C_∞	1.0 mol cm^{-3}	[2]
Electrons produced/reactant ion	n	2	[2]
Cell geometry dependent constant	q	$0<q<1$	–
Universal gas constant	R	8.314 J mol^{-1}K^{-1}	–
Faraday's constant	F	96,487 C mol^{-1}	–

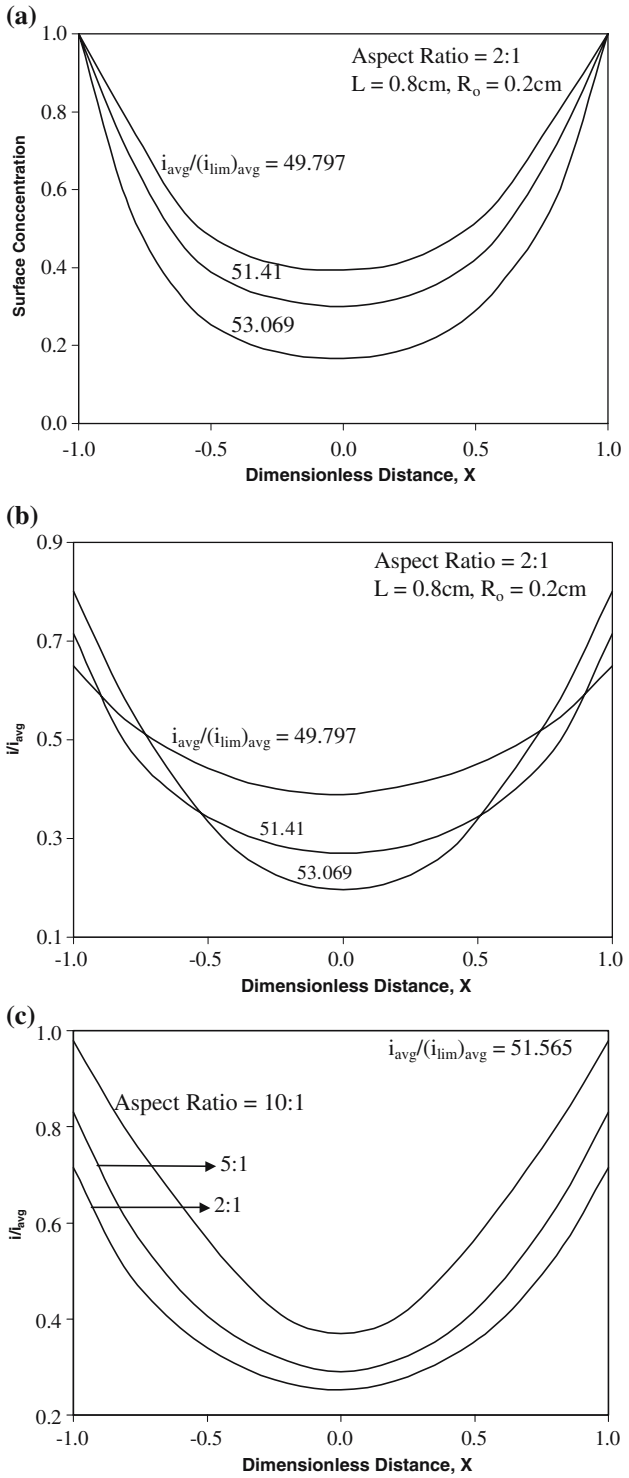

Fig. 6. (a) Calculated surface concentration distributions within a through-hole; (b) Distribution of current density within a through-hole at various levels of polarization; and (c) Dependence of the current density distribution on the through-hole geometry, R_0/L.

distribution [16–18]. We consider the flow between planar electrodes in the walls of a flow channel as shown in Figure 7. The boundary conditions at the insulating walls and at the anode ($y = b$) are the same as in earlier cases, while the boundary conditions at the cathode ($y = 0$) is

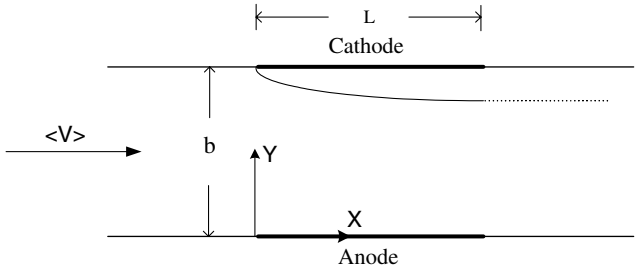

Fig. 7. Location of the plane-parallel electrodes on the walls of flow channel.

$$\frac{\partial C}{\partial y} = \frac{i}{nFD} \quad \text{at } y = 0 \ \text{ for } 0 < x < L \tag{28}$$

Using the same series solution assumption Eq. (26), the resulting equation for the surface concentration is

$$i^* = N \int_0^X \left(\frac{\mathrm{d}C_s^*}{\mathrm{d}X}\right)_{X=t} \frac{\mathrm{d}t}{\sqrt{[3]X - t}} = N \sum_{n=1}^{\infty} \frac{n}{3} a_n X^{\frac{n-1}{3}} \beta\left(\frac{n}{3}, \frac{2}{3}\right) \tag{29a}$$

where

$$N = \frac{n^2 F^2 D C_\infty}{(1-t)RTk} \frac{1}{\Gamma\left(\frac{4}{3}\right)} \left(\frac{2\langle U\rangle L^2}{3Db}\right)^{\frac{1}{3}} \tag{29b}$$

For this geometry the Laplace equation is subjected to the following conditions

$$\frac{\partial \phi}{\partial y} = 0 \quad \text{at } y = 0 \quad \text{for } x < 0 \,\&\, xL \tag{30}$$

$$\frac{\partial \phi}{\partial y} = \frac{-i}{k} \quad \text{at } y = 0 \quad \text{for } 0 < x < L \tag{31}$$

The model equations describing the cathode process are given in Table 3 and the simulation data in Table 4. To calculate the current density and concentration distributions on the two electrodes, two sets of five equations must be solved simultaneously along with the equality condition for anodic and cathodic current density distributions. The total current flowing through the reactor is given by

$$\int_0^1 i^*_{\text{cath}}(X)\mathrm{d}X + \int_0^1 i^*_{\text{anode}}(X)\mathrm{d}X = 0 \tag{32}$$

A design procedure can be readily set up for the above system. The parameters to be specified are N, J, b^* along with kinetic parameters. The current distributions are then determined for various applied voltages. But here in this particular case, this should to be done for both anode and cathode, so that the iteration continues until Eq. (32) is satisfied. This is done by running the

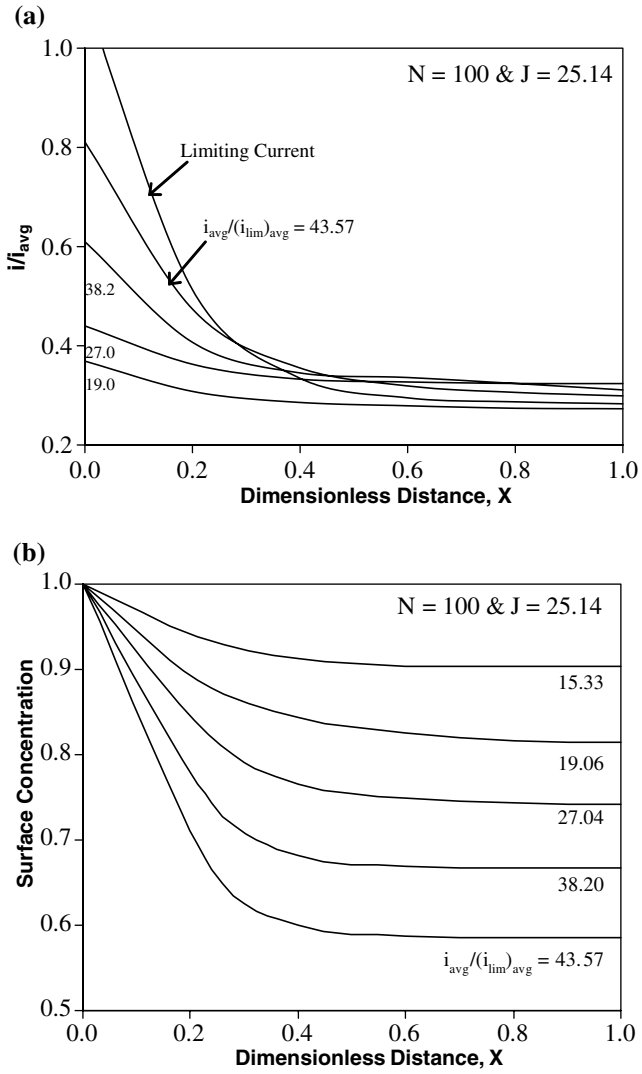

Fig. 8. (a) Cathodic current distribution for a fast reaction occurring at various average current densities and (b) Surface concentration distribution on the cathode.

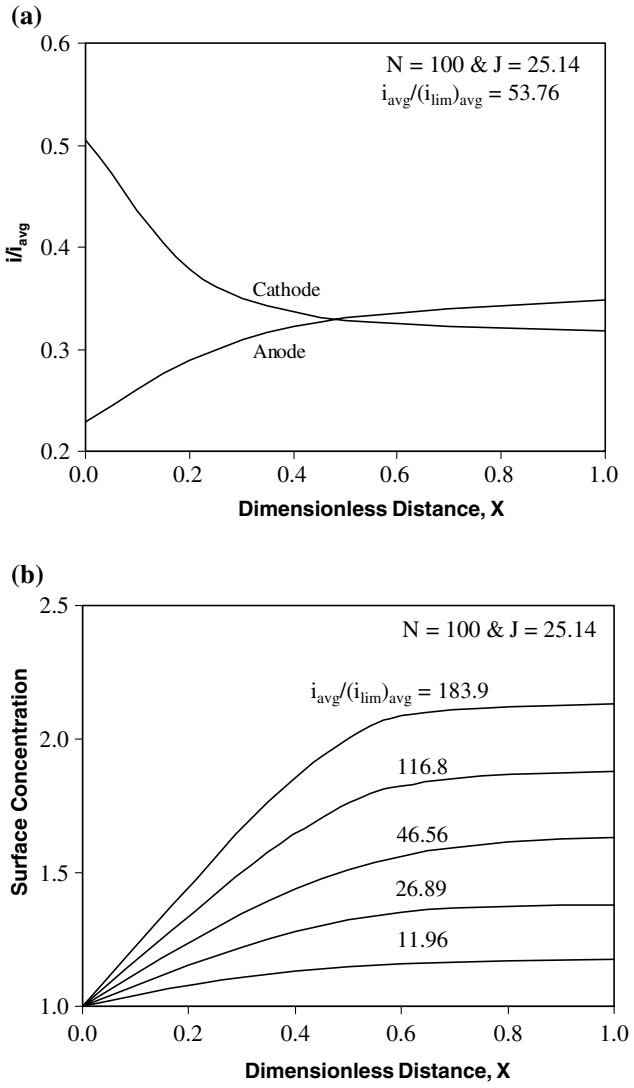

Fig. 9. (a) Comparison of anodic and cathodic current distributions and (b) Surface concentration distribution on the anode.

algorithm separately one anode and cathode and verify in the validity of Eq. (32) at the output level. The limiting current occurs when the current distribution is limited by mass transfer through the diffusion layer and is given by

$$i^*_{\text{lim}} = \frac{N}{X^{1/3}} \tag{33}$$

Figure 8a shows the current distribution for $N=100$ and $J=8\pi$ (this corresponds to Wagner parameter 4π) at various fractions of the limiting current; also shown is the limiting current density profile. Near the front of each electrode, the current drops rapidly, behaving like a secondary current distribution. However on the cathode, mass transfer effects become more important with increasing x/L. The concentration profiles for the cathode are shown in Figure 8b, the cathodic current cannot continue to behave like a secondary current because the reactant concentration has been reduced inside the diffusion layer. But concentration effects are relatively unimportant on the anode, and the anodic current continues to resemble a secondary current distribution. The interaction between the two electrodes through the Laplace equation is very apparent for the case of $h/L=0.5$. This behavior is caused at very high current density due to rapid depletion of reactant. However, after the current has dropped, the concentration decreases again. A similar but opposite behavior occurs on the anode as shown in Figure 9a and 9b. A comparison of anodic and cathodic current distributions is in harmony with the observation that large values of conductivity, and hence small values of N and i^*_{avg}, mean that the electrodes behave independently since they are coupled only through the ohmic potential drop. It is also found that, at a given fraction of the limiting current, the current distribution becomes less uniform with increasing N. For an infinite value of conductivity, the problem is similar to one of mass transfer and non-electrochemical catalysis.

5. Conclusion

A semi-analytical method that calculates the simplified tertiary current density distribution and concentration profiles of an electrochemical cell is presented. The method requires only an assumption of appropriate power series to solve for steady state laminar convective diffusion. Moreover, within the context of its limitations this computational method can be extended to treat various cell operational modes. Three test problems from classical electrochemical engineering are solved and discussed. The results are shown as functions of various current levels and electrode positions. Profiles of surface concentration and current density distribution on the electrode are computed by considering concentration polarization, activation polarization and ohmic potential drop in the electrolyte. The method for solving the governing equations utilizes the analytical solution to the maximum possible extent.

Acknowledgements

A research fellowship awarded to Dr. V. Boovaragavan, jointly from the Council of Scientific & Industrial Research, New Delhi, India, and Central Electrochemical Research Institute, Karaikudi, India, is gratefully acknowledged. Special thanks are due to Prof. A.K. Shukla, Central Electrochemical Research Institute, and Dr. Venkat R. Subramanian, Tennessee Technological University, USA, for their encouragement.

Appendix

The series solution assumption for the surface concentration on the continuous moving sheet electrode process is

$$C_s^* = \sum_{n=0}^{\infty} a_n X^{\frac{n}{2}} \qquad (A-1)$$

For this case Eq. (18) reads (here $q = 1/2$ & $a_0 = 1.0$)

$$i^* = N \int_0^X \left(\frac{dC_s^*}{dX}\right)_{X=t} \frac{dt}{\sqrt{X-t}} \qquad (A-2)$$

Using Eq. (A-1), we have from Eq. (A-2) that the local current density can be expressed in series form as

$$i^* = N \sum_{n=1}^{\infty} \frac{n}{2} a_n X^{\frac{n-1}{2}} \beta\left(\frac{n}{2}, \frac{1}{2}\right) \qquad (A-3)$$

Equation (5) reads

$$i^* = J C_s^{*\gamma} \left[\exp\left(\alpha \eta_a^*\right) - \exp\left(-\beta \eta_a^*\right)\right] \qquad (A-4)$$

Equating Eqs. (A-3) and (A-4) and then again equating the like terms of X we get expressions to evaluate the series coefficients.

$$J\left[\sum_{n=0}^{\infty} a_n X^{\frac{n}{2}}\right]^{\gamma} \left[\exp\left(\alpha \eta_a^*\right) - \exp\left(-\beta \eta_a^*\right)\right] = N \sum_{n=1}^{\infty} \frac{n}{2} a_n X^{\left(\frac{n-1}{2}\right)} \beta\left(\frac{1}{2}, \frac{n}{2}\right)$$

$$a_1 N \frac{1}{2} \beta\left(\frac{1}{2}, \frac{1}{2}\right) = J Y a_0^{\gamma} \qquad (A-5)$$

$$a_2 N \frac{1}{2} \beta\left(1, \frac{1}{2}\right) = \gamma J Y a_0^{\gamma-1} \frac{a_1}{2} \qquad (A-6)$$

$$a_3 \frac{3N}{2} \beta\left(\frac{3}{2}, \frac{1}{2}\right) = \gamma(\gamma-1) J Y a_0^{\gamma-2} \frac{a_1}{2} + \gamma J Y a_0^{\gamma-1} \frac{a_1}{2} \qquad (A-7)$$

$$a_4 \frac{3N}{2} \beta\left(2, \frac{1}{2}\right) = \gamma(\gamma-1)(\gamma-2) J Y a_0^{\gamma-3} \frac{a_1^3}{8} + 2\gamma(\gamma-1) J Y a_0^{\gamma-2} \frac{a_2}{2} + \gamma(\gamma-1) J Y a_0^{\gamma-1} \frac{a_1}{2} \frac{a_2}{2} + \gamma J Y a_0^{\gamma-1} \frac{3a_3}{4} \qquad (A-8)$$

where $Y = -\left\{\exp(\alpha \eta_a^*) - \exp(-\beta \eta_a^*)\right\}$. Assuming a value for activation polarization, the surface concentration can be calculated at any given position on the electrode using Eqs. (A-5) to (A-8) and $a_0 = 1.0$, this is a series evaluation. The corresponding local current density distribution is calculated from electrode kinetics Eq. (A-3). The concentration overpotential can be calculated from the Eq. (6). Next, using the evaluated current density, the ohmic potential drop can be computed from the analytical solution of the Laplace equation derived for the respective geometry. Next, with all the overpotentials in hand, the cell potential E^* is calculated based on the output from the initially guessed activation overpotential. If the absolute value of the relative percent difference between the calculated and specified cell potential is greater than the specified tolerance (10^{-4}) then the activation polarization is adjusted and the procedure repeated until convergence.

References

1. J. Newman, *Ind. Eng. Chem.* **60** (1968) 12.
2. J. Newman, *Electrochemical Systems* (Prentice Hall, Englewood Cliffs, NJ, 1991).
3. M.H. Chung, *Electrochim. Acta* **45** (2000) 3949.
4. V.R. Subramanian and R.E. White, *J. Electrochem. Soc.* **147** (2000) 1636.
5. V.R. Subramanian and R.E. White, *J. Electrochem. Soc.* **149** (2002) C498.
6. M. Georgiadou, *Electrochim. Acta* **48** (2003) 4089.

7. S.H. Chan and H.Y. Cheh, *Chem. Eng. Commun.* **191** (2004) 881.
8. B. Vijayasekaran and C.A. Basha, *Electrochim. Acta* **51** (2005) 200.
9. V. Boovaragavan and C.A. Basha, *Chem. Eng. J.* (2006) in press.
10. B. Vijayasekaran and C.A. Basha, *J. Power Sources* (2005) in press.
11. I. Rousar, V. Mejta and V. Cezner, *Chem. Eng. Sci.* **35** (1980) 717.
12. D. Pletcher and F.C. Walsh, *Industrial Electrochemistry* (Kluwer Academic Publishers, UK, 1994).
13. C.F. Coombs, *Coombs*' Printed Circuits Handbook, 5th ed., (McGraw-Hill Professional, New York, 2001).
14. C. Fu, C. Ume, L. David and McDowell, *Finite Element Anal. Des.* **30** (1998) 1.
15. R.B. Bird, W.E. Stewart and E.N. Lightfoot, *Transport Phenomena* (Wiley, New York, 1960).
16. J.M. Bisang, *J. Appl. Electrochem.* **27** (1997) 379.
17. G. Nelissen, A. Van Theemsche, C. Dan, B. Van den Bossche and J. Deconinck, *J. Electroanal. Chem.* **563** (2004) 213.
18. A.A. Wragg and A.A. Leontaritis, *Chem. Eng. J.* **66** (1997) 1.